TECHNICAL MEMORANDUMS

NATIONAL ADVISORY COMMITTEE FOR AERONAUTICS

715

PRESSURE AND FRICTIONAL RESISTANCE OF A CYLINDER AT REYNOLDS NUMBERS 5,000 TO 40,000

By L. Schiller and W. Linke

Zeitschrift für Flugtechnik und Motorluftschiffahrt
Vol. 24, No. 7, April 13, 1933
Verlag von R. Oldenbourg, München und Berlin

Washington
July 1933

NATIONAL ADVISORY COMMITTEE FOR AERONAUTICS

TECHNICAL MEMORANDUM NO. 715

PRESSURE AND FRICTIONAL RESISTANCE OF A CYLINDER AT REYNOLDS NUMBERS 5,000 TO 40,000

By L. Schiller and W. Linke

SUMMARY

1. This report presents the results of a series of free-jet measurements to determine the pure frictional resistance of a cylinder from the difference between total resistance and pressure at Reynolds Numbers 5,000 to 40,700.

2. The skin friction is 5 percent of the total resistance at Re = 5,000, and has dropped to 2 percent at Re = 40,000, which supports Thom's theory.

3. The pressure indication of an orifice in the cylinder wall within range of the adhering boundary layer is exaggerated proportionally to the orifice diameter and to the tangential pressure gradient.

4. Conformably to the rise in drag coefficient at Re $\cong$ 2,000 to Re $\cong$ 20,000, there is a progressive transformation of the "dead air space" and approach of a critical point on the cylinder which denotes the end of the laminar mixing zone.

5. Wires introduced in the laminar transition zone render it turbulent and cause a much quicker change into the squared resistance zone than with the bare cylinder.

---

*"Druck- und Reibungswiderstand des Zylinders bei Reynoldsschen Zahlen 5000 bis 40000." Z.F.M., April 13, 1933, pp. 193-198.

INTRODUCTION

The total resistance W_g of a body to flow can be divided into pressure W_p and friction W_r:

$$W_g = W_p + W_r \qquad (1)$$

The former (W_p) is given by the vector sum of the normal forces on the individual surface elements, the latter (W_r) by that of the tangential forces. Both quotas are contingent upon the shape of the body and fluctuate within large limits: A plate exposed to horizontal flow manifests almost exclusively, frictional resistance, whereas a plate in a vertical flow evinces primarily, pressure. The first case is very similar to that of slender airfoils at small angles of attack;* the second, to flow around spheres and to cylinders in transverse flow. The pressure is measured on suitably arranged orifices. The frictional resistance is, according to formula (1), obtained as difference between the total resistance and the pressure. The friction quota being very small for spheres and cylinders, its determination demands very precise total resistance and pressure measurements. In particular, both measurements must be effected on the same object and with the same arrangement at the same flow attitude. Such measurements were lacking for the cylinder. Ermisch (reference 1) defined the frictional resistance from his own pressure and Wieselsberger's total resistance measurements at improbably high values. (Compare fig. 2.) Thom (reference 2) chose to combine his own pressure measurements with Relf's findings, for which reason it was deemed advisable first, according to Mr. Flachsbart, who had made similar measurements, to effect such measurements in a test set-up with the same cylinder, in order to definitely establish the true frictional drag.

Concurrently our measurements were intended to check one theoretical expression by Thom (reference 3) by an improved test. Dr. Thom arrived at a solution of the boundary layer equations in closed form. These velocity profiles are in close agreement with the experiments from the forward stagnation point ($\theta = 0^\circ$) to $\theta = 60^\circ$. The friction $f = \mu \left(\frac{\partial u}{\partial y}\right)_{y=0}$ (u = tangential velocity, y = vertical dis-

*Vgl. Ergebn. d. Aerodyn. Vers.-Anst. 3, 87, 1927.

tance from cylinder surface is

$$f = \frac{\rho}{2} w^2 \sqrt{\frac{1}{Re} \Psi \left(p_1, \frac{dp_1}{d\theta}, \frac{d^2 p_1}{d\theta^2} \right)} \qquad (2)$$

wherein ρ = fluid density, w = velocity of flow, $Re = \frac{w D}{\nu}$ with D = cylinder diameter and $\nu = \frac{\mu}{\rho}$ = kinematic viscosity. The Reynolds Number $p_1 = \frac{p - p_o}{\frac{\rho}{2} w^2}$ is the difference between pressure p on the surface for angle θ and pressure p_o of the undisturbed flow measured in fractions of dynamic pressure; Ψ is a function of the cited quantities. For the integration from 0 to 60°, Thom used equation (2), from 60 to 90° the experimental velocity profiles, and thus obtained, in so far as attributable to pure frictional drag of the front half, the coefficient of friction

$$c_r = 3.84 \sqrt{\frac{1}{Re}} \qquad (3)$$

($W_r = c_r F \frac{\rho}{2} w^2$, F = projection of cylinder onto a plane perpendicular to the direction of flow.) With an increment for the admittedly small friction of the rear half, Dr. Thom puts the approximate value at

$$c_r = 4 \sqrt{\frac{1}{Re}} \qquad (4)$$

Thom's own experiments ranged from $Re = 28$ to 17,000, of which only two points exceeded 8,000 (fig. 2). It was therefore desirable to raise the number of test points by increased measuring accuracy and to extend the range to higher Re (which is more difficult because of the decreasing skin friction). This was separately effected for the transition zone from $c_{g\,min}$ at $Re = 2000$ up to the squared zone.

Hereby it was found that the rise of c_g is accompanied by systematic changes of pressure distribution, for which reason the flow and pressure field downstream from the cylinder was made the subject of a special investigation.

ANALYSIS OF COEFFICIENT OF FRICTION c_r

The tests were made in a circular air stream (ϕ = 60 cm (23.6 in.) local speed changes ±0.3 percent). Two fixed, upright plates ensured that the flow around the cylinder was two-dimensional.

To measure the total drag on the two-component scale the cylinder had to be movable through the plates, which necessitated "scaling" with very little clearance space. Plate boundary layer effects were allowed for separately. A detailed description of this experimental set-up is given in reference 4.

For measuring the pressure, the cylinder had an orifice in a middle section and the different angles θ (starting from stagnation point) were obtained by turning the cylinder, which at the same time also served as pressure pipe. The effect of size of the pressure orifice on the pressure indications is shown in the following section.

The measurements were made on five cylinders (D = 1.00, 1.39, 2.00, 3.00, 4.00 cm (0.39, 0.55, 0.79, 1.18, and 1.57 in., respectively)), at Reynolds Numbers of 5,000 to 41,000. The different diameters served in part for extending the measuring range, and in part as check that the finite jet diameter did not exert any perceptible effect. Figure 1 shows c_g and c_p for D = 1 cm (0.39 in.) and 4 cm (1.57 in.) and of a portion for 2 cm (0.79 in.), together with Relf and Wieselsberger's c_g data. There are no marked discrepancies between the c_g curves except at Re between minimum and the squared range. Another graph (not shown here) reveals that in the squared range the c_g and c_p curves follow each other for different cylinders and cover each other at equal Re* but that it is not wholly complete in the transition zone. Evidently small infractions against similarity exist there already, although this does not recur in the c_r diagram when the difference is formed between two curves of one cylinder.

Figure 2 gives the results for c_r. The minor discrepancies between c_r curves are within accuracy of measurement. At Re = 5,000 (log Re = 3.7) the frictional resist-

---

*Which proves that the boundaries of the air jet exert no effect on the resistance.

ance is 5 percent of the total resistance ($c_g = 0.94$) and at $R_\varrho = 40{,}000$ ($\log R_\varrho = 4.6$) it has dropped to 2 percent ($c_g = 1.19$).

The discrepancy of our figures from Thom's formula (4) averages ±10 percent. (See fig. 2.) These differences, which amount to ~ 0.5 percent of the total resistance, lie within measuring accuracy. The comparison supports therefore Dr. Thom's theory of the coefficient of friction up to the squared range. Figure 2 also shows the points of Thom-Relf and Ermisch-Wieselsberger, of which the latter in particular are at variance with our measurements and with the theory.

As concerns the correlation between friction and character of flow, it seems that c_r reaches a certain minimum in the squared range, which changes very little as yet, whereas at smaller R_ϱ, where the gradient of c_r is stronger, the changes in the pressure and in the whole flow form are substantially greater. This is already indicated by the pressure distribution on the surface (fig. 3). Aside from a general increase in negative pressure at increasing R_ϱ, there is a pressure minimum at $\theta = 180^\circ$. The transformation occurs perfectly parallel to the rise in the resistance factors; at around $R_\varrho = 25{,}000$, the pressure distribution has reached a definite form.

PRESSURE INDICATION AND ORIFICE DIAMETER

Thom's experiments covered the range between $\theta = 0^\circ$ and $\theta = 70^\circ$ (reference 2). According to them the pressure distributions measured on a cylinder with orifices of different diameter h, can be made to agree when

$$\theta = \theta_0 - \frac{1}{2}\frac{h}{D} \qquad (5)$$

but not by coordinating the measured pressures with the center of the orifice, i.e., angle θ_0. Similar experiments of our own were calculated to check the applicability of equation (5) to our pressure-distribution measurements with 12 different holes (h = 0.195 mm (0.008 in.) to 3.04 mm (0.12 in.)) at $R_\varrho = 6{,}800$ and $R_\varrho = 11{,}650$ (D = 1 cm (0.39 in.)). The interpretation of θ between 0° and 72° (point of separation) revealed a linear interdependence between h and the pressure indication. (See

fig. 4, which gives the measured values for $\theta = 30^\circ$ non-dimensionally.)

The coefficient A, that is, the inclination, varies as θ. It is given in table I. No systematic relationship is ascertainable for $\theta > 72^\circ$.

TABLE I

θ°	A	$\frac{dq^a}{d\theta}$	$B = \frac{A}{\frac{dq^a}{d\theta}}$
0	0.00	0.0	-
10	0.30	0.7	0.43
20	0.72	1.8	0.40
30	1.035	2.3	0.45
40	1.18	2.8	0.42
50	1.13	2.4	0.47
60	0.525	1.3	0.40
72	0.00	0.0	-

With the assumption that the extrapolation according to $h = 0$ gives the true pressure, the error Δq^a, when $q^a = \frac{p - p_o}{\frac{\rho}{2} w^2}$, is

$$\Delta q^a = q^a_{\text{measured}} - q^a_{\text{true}} = A \frac{h}{D} \qquad (6)$$

A comparison of A with the pressure gradients $\frac{dq^a}{d\theta}$ prevailing at the same θ shows approximate proportionaility. Thus with $A = B\frac{dq^a}{d\theta}$ the approximation may be expressed by

$$\Delta q^a = B \frac{dq^a}{d\theta} \frac{h}{D} \qquad (7)$$

A similar relationship may possibly be valid for other cases also (airship bodies, etc.). With smaller orifice diameters our correction reverts to Thom's correction (equation 5). In figure 5, I is the measured curve and II the

correct curve. For small orifices

$$\frac{\Delta q^a}{\Delta \theta} = \frac{dq^a}{d\theta} \tag{8}$$

and from (7) follows

$$\Delta \theta = B \frac{h}{D}. \tag{9}$$

But according to table I, B = 0.43, that is, not very much different from Thom's value, 0.5.

Equation (9) signifies: One obtains the point at which the measured pressure is the true pressure when reducing the measured angle by 0.43 times the amount of the "relative orifice diameter."

FIELD OF PRESSURE BEHIND CYLINDER

According to a previous section (pages 4 and 5), the pressure distribution changes appreciably within the range of Reynolds Numbers in which c_g increases. Presumably this transformation is related to processes in the zones in which the transition from undisturbed flow to dead air space occurs. For the squared range these transitory zones are, according to Fage and Johansen (reference 5), turbulent mixing zones emanating from the region of the equator. They approximately follow the Tollmien-Prandtl mixing theory.

In order to establish the connections at smaller Re, we must first define the process of the transition zone, or as we shall call it, the "mixing zone."* Within this zone the velocity drops from constant to zero in the outside flow or to a very small value in the dead air space. Since the pressure in the latter is negative, the pressure indication of a Pitot tube mounted parallel to the main flow direction - introduced from without through the mixing zone into the dead air space - progresses from constant pressure values to lower amounts. Owing to the difficulties involved in effecting accurate static pressure and velocity records in such zones (reference 6), the said

*Without, however, maintaining that there is any turbulent mixing in it.

pressure measurements were merely used to define the boundaries of the mixing zone. The pressure behind two cylinders (D = 1.4 cm (0.55 in.) and D = 2.0 cm (0.79 in.)) is determined on straight lines y, perpendicular to the direction of flow at various distances x from the cylinder. Figure 6 shows the profiles measured for R_Q = 8,540 and D = 1.4 cm (0.55 in.) up to symmetrical axis s through the center of the cylinder. The points A in which the pressure p' begins to drop, and the points B, where a constant minimum value is reached, define the boundaries of the mixing zone.

Check tests with a Pitot tube set at 15° to the undisturbed flow disclosed that, independent of possible flow errors, the measurements give the correct total pressure (up to a constant).

The projected pieces A-B (fig. 6) in direction y, that is, the widths of the mixing zones, plotted for the different spacings x, afford diagrams such as those shown in figures 7, 8, and 9 for D = 1.4 cm (0.55 in.) at three different R_e.

At R_Q = 5,000 (fig. 7) the mixing zone increases only gradually in width at first, the expansion does not become appreciable until about $\frac{1}{2}$ D behind the cylinder so that the symmetrical axis s (E) is reached at 1 D. The expanse of the dead air space is comparatively large.

Beginning at the cylinder the pressure p' in the symmetrical axis s has at first a constant value which corresponds to that of the cylinder orifice at $\theta = 180°$. (Compare fig. 3, R_e = 5,000.) Beginning at distance $\sim\frac{1}{2}$ D conformably to the course of the mixing zone, pressure p' drops in direction of x. As a result, the pressure has the same value (fig. 6) within the dead air space on a line y perpendicular to x, but not for different x. Somewhat downstream from the dead air end E a minimum is reached at F.

As R_Q increases (figs. 7, 8, and 9) the dead air changes from a large, long extended zone into a small, more pointed zone; or, in other words, the point of the noticeable expansion of the mixing zone shifts upstream as R_e increases. The closer it approaches the equator, the more the form of the mixing assumes the symmetrical shape of a wedge.

Figure 10 shows the dead air lengths e, defined by the points E, plotted against the Reynolds Number. They seem to strive toward a constant value of $e \cong D/2$; that is, the character of the flow approaches permanency, as anticipated.

Figure 10 also shows the distances f, of the above-mentioned pressure minima from the cylinder. The parallelism of the curves signifies that changes in f likewise represent a criterion for the transformation of the flow.

For interpreting the described changes of the pressure pattern δ/D (δ = thickness of mixing zone) may be plotted against x/D or $Re_\delta = \delta w/\nu$ may be plotted versus $Re_x = xw/\nu$. The null point for the x values is taken at $\theta = 45^\circ$ in figure 11. With this choice of null point the Re_δ are approximately coincident on one curve for the different Reynolds Numbers. Furthermore, at small Re, Re_δ, and Re_x or in a different representation at small Re, δ/D, and x/D, the individual curves assume a form which follows the power law:

$$Re_\delta = \text{const} \sqrt{Re_x} \quad \text{or} \quad \frac{\delta}{D} = \text{const} \sqrt{\frac{x}{D}} \tag{10}$$

Since these laws, conformably to Prandtl's boundary layer theory, represent characteristic relations for laminar boundary layers, whereas our mixing zones may equally be considered detached, free boundary layers, the existence of equations (10) can be taken as proof of the laminar character of the mixing zone. The points diverging from equation (10) are given as critical Reynolds Numbers in table II. The last column shows that the critical points approach the cylinder as Re increases; the turbulent mixing zone displaces the laminar piece more and more, the turbulent interferences advance toward the cylinder and have perhaps reached it at the beginning of the squared zone.

TABLE II

Curve	Re	w cm/s	D cm	$Re_{\delta crit}$	$Re_{x\ crit}$	$\left(\frac{x}{D}\right)_{crit} = \frac{Re_{x\ crit}}{Re}$
I	14,480	1,510	1.4	-	-	-
II	12,410	867	2.0	-	-	-
III	8,540	897	1.4	900	6,000	0.70
IV	6,290	434	2.0	730	5,600	0.89
V	5,000	518	1.4	650	5,200	1.04
VI	3,540	244	2.0	510	5,000	1.41

EXPERIMENTS WITH ARTIFICIAL TURBULENCE OF THE "FREE" BOUNDARY LAYER

The described development in the range of Re = 3,000 to Re = 15,000 can be considerably accelerated by the use of thin wires on the surface of the cylinder at, or in front of the equator, as illustrated by the displacement of the pressure minimum (f = its distance from cylinder) toward the cylinder in figure 12. Figure 13 shows the simultaneous steep rise in c_g (with a wire of d = 0.3 mm (0.012 in.) diameter at the equator of the D = 1.4 cm (0.55 in.) cylinder).

These experiments are analogous to those of Prandtl (reference 7), in which at higher Re the change to lower drag coefficients was speeded up by wires, as manifested by the incipient turbulence of the boundary layer around the sphere. In contrast to that, ours is manifestly a problem of incipient turbulence of the detached "free" boundary layer. At the higher Reynolds Numbers of the Prandtl experiments it might, according to the above results regarding the advancing turbulence toward the cylinder, be totally turbulent, so that the wire ring at the equator remained ineffective up to around Re = 180,000. But at our small Re the free boundary layer is laminar and becomes laminar because of the wire, which stipulates the increased drag. A visible proof is given in figure 12.

The wire d = 0.1 mm (0.004 in.) placed at 90°, evinces but a minor effect, whereas, when shifted into the free boundary layer (0.2 mm) (0.008 in.) away from cylinder), the change is complete.

Translation by J. Vanier,
National Advisory Committee
for Aeronautics.

REFERENCES

1. Ermisch, H.: Abh, a.d. Aerodyn. Inst. Aachen 6, 18, 1927.

2. Thom, A.: An Investigation of Fluid Flow in Two Dimensions. R. & M. No. 1194, British A.R.C., 1929.

3. Thom, A.: The Boundary Layer of the Front Portion of a Cylinder. R. & M. No. 1176, British A.R.C., 1928.

4. Linke, W.: Phys. Zeitschr. 32, 900, 1931.

5. Fage, A., and Johansen, F. C.: Phil. Mag. (7) 5, 417, 1928.

6. Schlichting, H.: Ing. Arch. 1, 568, 1930.

7. Prandtl, L.: Gött. Nachr. 1914, p. 177.

Figs. 1,2,3,4,5

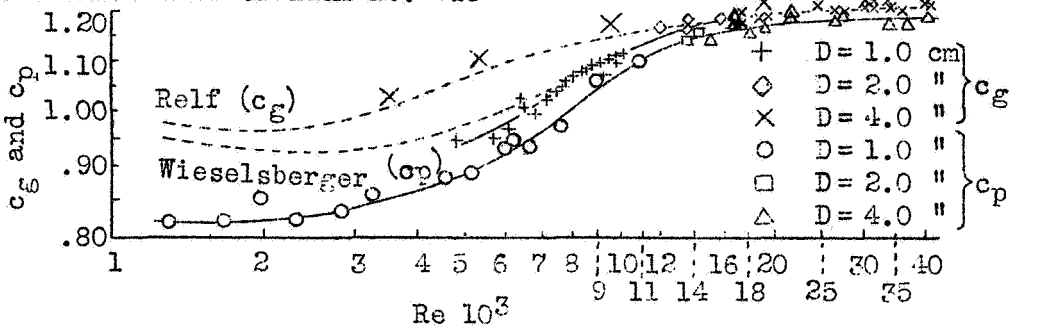

Figure 1

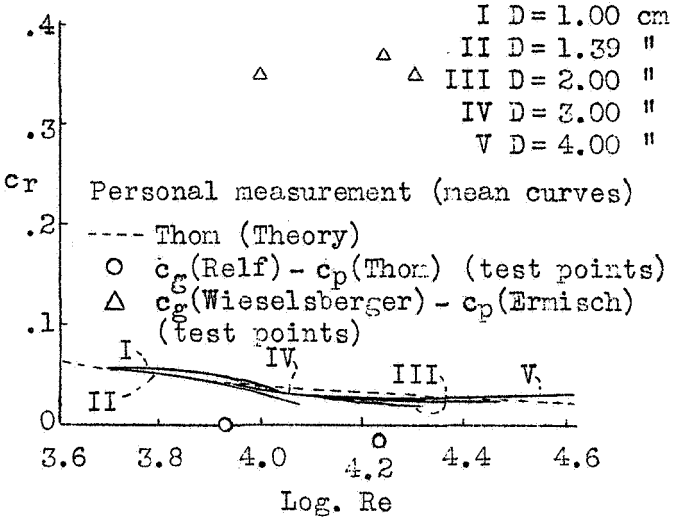

Figure 2

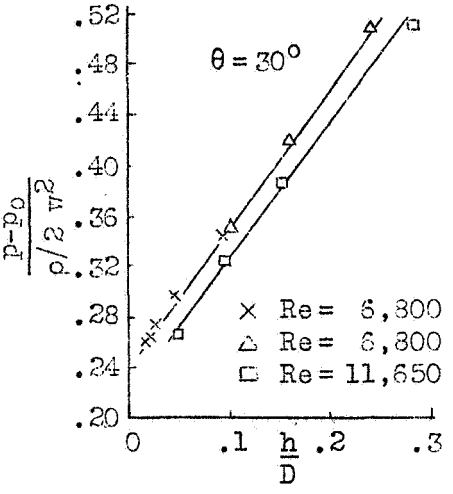

Figure 4

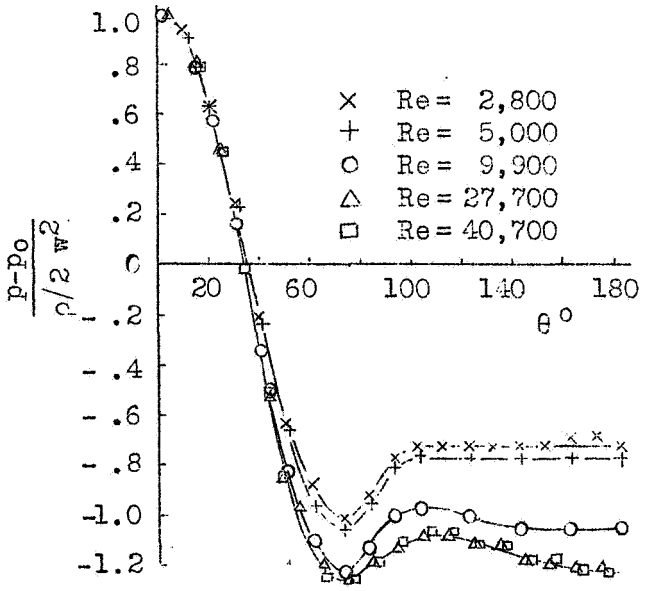

Figure 3

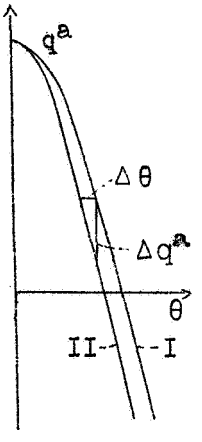

Figure 5

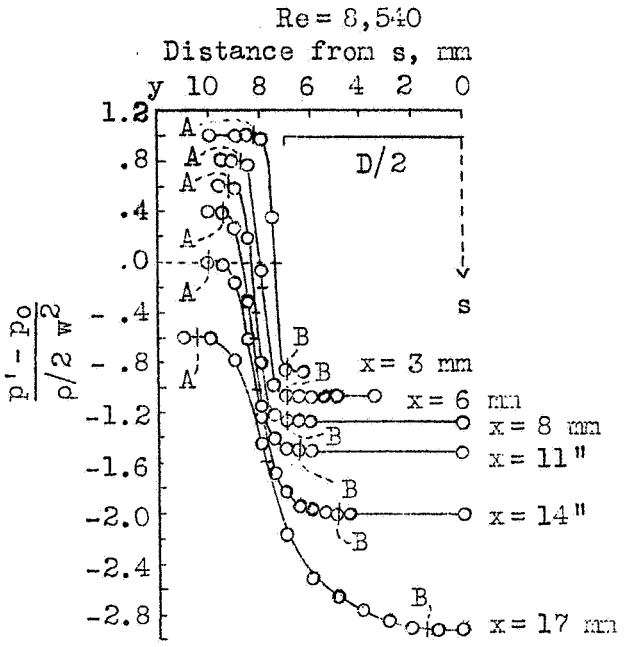

x measured from equator of cylinder

Figure 6

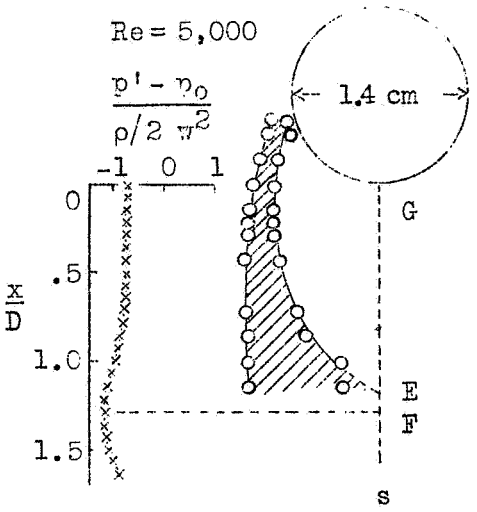

x=distance from cylinder

Figure 7

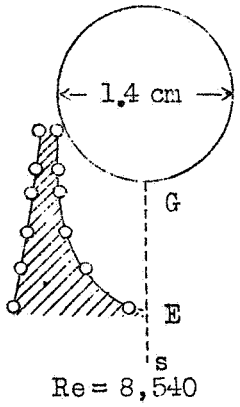

Re = 8,540

Figure 8

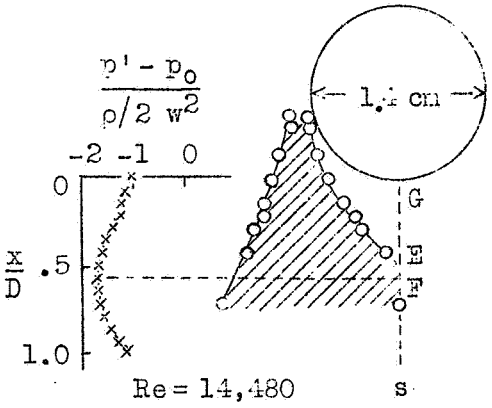

Re = 14,480

Figure 9

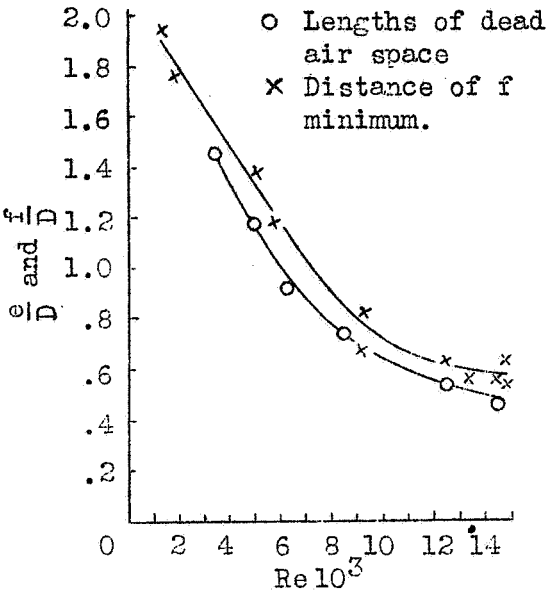

Figure 10

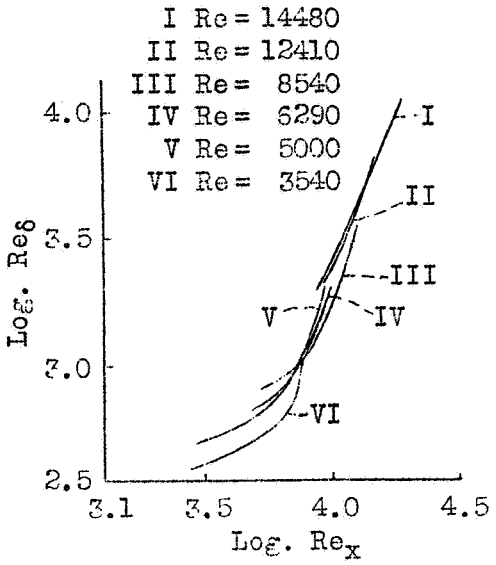

Figure 11

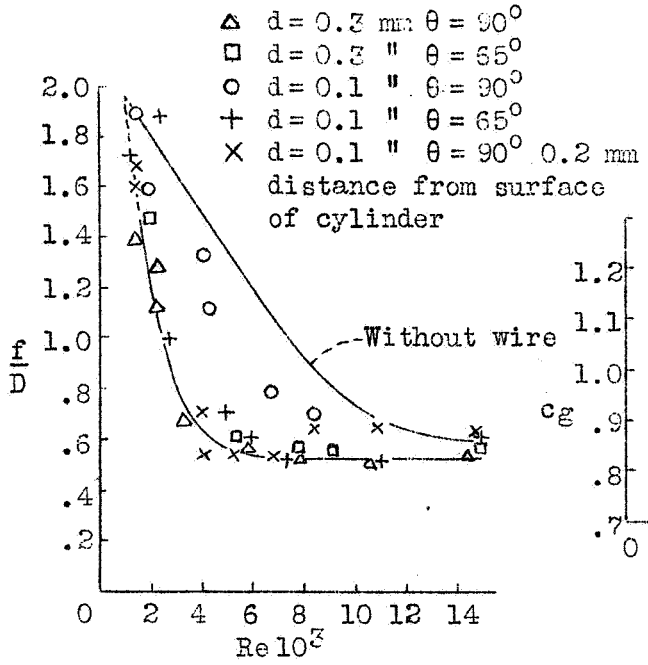

Figure 12

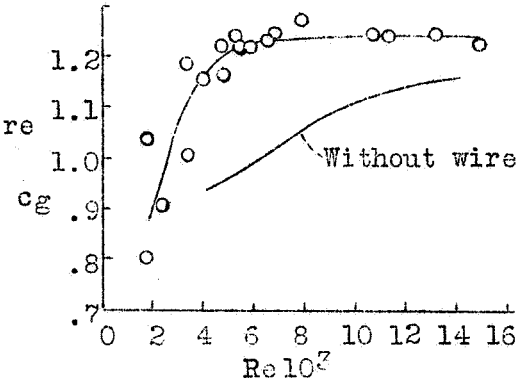

Figure 13